Influenza A(H5N1) Virus Infections in 2 Free-Ranging Black Bears (*Ursus americanus*), Quebec, Canada

Benjamin T. Jakobek, Yohannes Berhane, Marie-Soleil Nadeau, Carissa Embury-Hyatt, Oliver Lung, Wanhong Xu, Stéphane Lair

Wholly Eurasian highly pathogenic avian influenza H5N1 clade 2.3.4.4b virus was isolated from 2 free-ranging black bears with meningoencephalitis in Quebec, Canada. We found that isolates from both animals had the D701N mutation in the polymerase basic 2 gene, previously known to promote adaptation of H5N1 viruses to mammal hosts.

Since its arrival in North America during December 2021, the Eurasian highly pathogenic avian influenza (HPAI) virus subtype H5N1, clade 2.3.4.4b, has been associated with a high mortality rate for wild birds all over the continent (*1*). Affected bird species include mainly waterfowl and colonial nesting marine birds, as well as scavenger birds, such as gulls, eagles, vultures, and corvids (*2*,*3*). As with several other subtypes, HPAI H5N1 can potentially infect persons, although clinical cases in humans have been limited (*4*). However, this virus has been shown to be pathogenic for different species of wild mammals, including red fox, striped skunk, mink, raccoon, and seals (*5*–*7*). Infections with influenza A(H1N1) viruses have been described in captive sloth bears (*8*). We report and describe infections by HPAI H5N1 virus in 2 black bears (*Ursus americanus*) found in Quebec, Canada, during the summer of 2022.

Author affiliations: Centre Québécois sur la Santé des Animaux Sauvages/Canadian Wildlife Health Cooperative, St. Hyacinthe, Quebec, Canada (B.T. Jakobek, S. Lair); Université de Montréal, St. Hyacinthe (B.T. Jakobek, S. Lair); University of Saskatchewan Western College of Veterinary Medicine, Saskatoon, Saskatchewan, Canada (Y. Berhane); Canadian Food Inspection Agency National Centre for Foreign Animal Disease, Winnipeg, Manitoba, Canada (Y. Berhane, C. Embury-Hyatt, O. Lung, W. Xu); University of Manitoba, Winnipeg (Y. Berhane, O. Lung); Ministère de l'Agriculture, des Pêcheries et de l'Alimentation Laboratoire de Santé Animale, St. Hyacinthe (M.-S. Nadeau)

DOI: https://doi.org/10.3201/eid2910.230548

The Study

Two young-of-the-year black bear cubs (likely born in January–February) were observed wandering on a road within the Forillon National Park in Gaspé, Quebec, Canada (48°51′39″N, 64°13′26″W), on June 14, 2022. The cubs, which were active and quite vocal, were not attended by their dam. Shortly afterward, an adult female bear with unusual behavior was reported ≈200 m from the cubs. This female was wandering between vehicles, fell into a river, and began circling. Upon the arrival of park officials, the animal was in lateral recumbency and convulsing in a ditch.

Because of the severity of the neurologic signs present and concern for public safety, the bear was anesthetized and then euthanized. The 2 cubs, presumed to be orphaned, were also euthanized. The carcasses of the adult female and 1 of the cubs were subsequently frozen. The adult female was thawed a few days later and examined on site. Different organs were sampled, refrozen and shipped, along with the originally frozen cub, to the Canadian Wildlife Health Cooperative Quebec regional center for further macroscopic examination, which was performed on July 7, 2022.

Macroscopic examination of viscera of the adult female show no notable findings, other than extensive postmortem changes. The cub (a 5.1-kg female) was thin and had limited fat stores. A mild mesenteric lymphadenomegaly was present, and the cerebrum appeared to be diffusely congested.

Histopathologic examination of tissues sampled from the adult female showed multifocal infiltration of the meninges by numerous lymphoplasmacytic cells, which extended into the Virchow–Robin spaces, forming perivascular cuffing. Neuronal necrosis associated with satellitosis and glial nodules was commonly observed. Aggregates of polymorphonuclear cells in the cerebral substance and areas of neuropile vacuolization with axonal degeneration were also present. The cub had similar, but of lower intensity and predominantly neutrophilic in nature, cerebral inflammatory and degenerative lesions, in addition to fibrinoid neutrophilic vasculitis. Small necrotic foci surrounded by granulocytes and mononuclear cells were also occasionally seen in the liver of the cub.

Influenza A virus (IAV) antigen was detected by using immunohistochemical staining (Appendix, https://wwwnc.cdc.gov/EID/article/29/10/23-0548-App1.pdf) in brain and liver cells; liver cells were observed only in the bear cub (Figure 1). Brain tissues from both animals were negative for rabies virus by the direct rapid immunohistochemical test (*9*).

We extracted RNAs from brain tissues and tracheo-rectal swab specimens from both animals and found that they were positive for IAV genomic material by using matrix and H5 gene specific real-time reverse transcription PCRs (*10*,*11*). We isolated H5N1 viruses from brain samples collected from both bears in 9-day-old embryonated specific pathogen-free chicken eggs. We amplified all 8 genome segments of the virus directly from clinical samples and isolates and were sequenced by using the Oxford Nanopore platform as described (*12*), and the Rapid Barcoding Kit 96 (https://www.nanoporetech.com). We basecalled raw Nanopore signal data and demultiplexed with Guppy v5.1.12 (https://timkahlke.github.io) using the super-accurate basecalling model. We then analyzed and assembled the basecalled reads by using the CFIA-NCFAD/nf-flu v3.1.0 (https://zenodo.org/record/7011213#.ZBs5cXbMIuU) nextflow workflow.

The hemagglutinin (HA) gene of the virus belonged to Eurasian goose/Guangdong (Gs/GD) lineage HPAI H5N1 clade 2.3.4.4b and had the cleavage site motif of PLREKRRKR/GLF, compatible with HPAI viruses (Figure 2). All 8 genome segments of the viruses from both bears contained wholly Eurasian IAVs similar to the Newfoundland-like H5N1 viruses, which came from Europe to Canada by the Atlantic

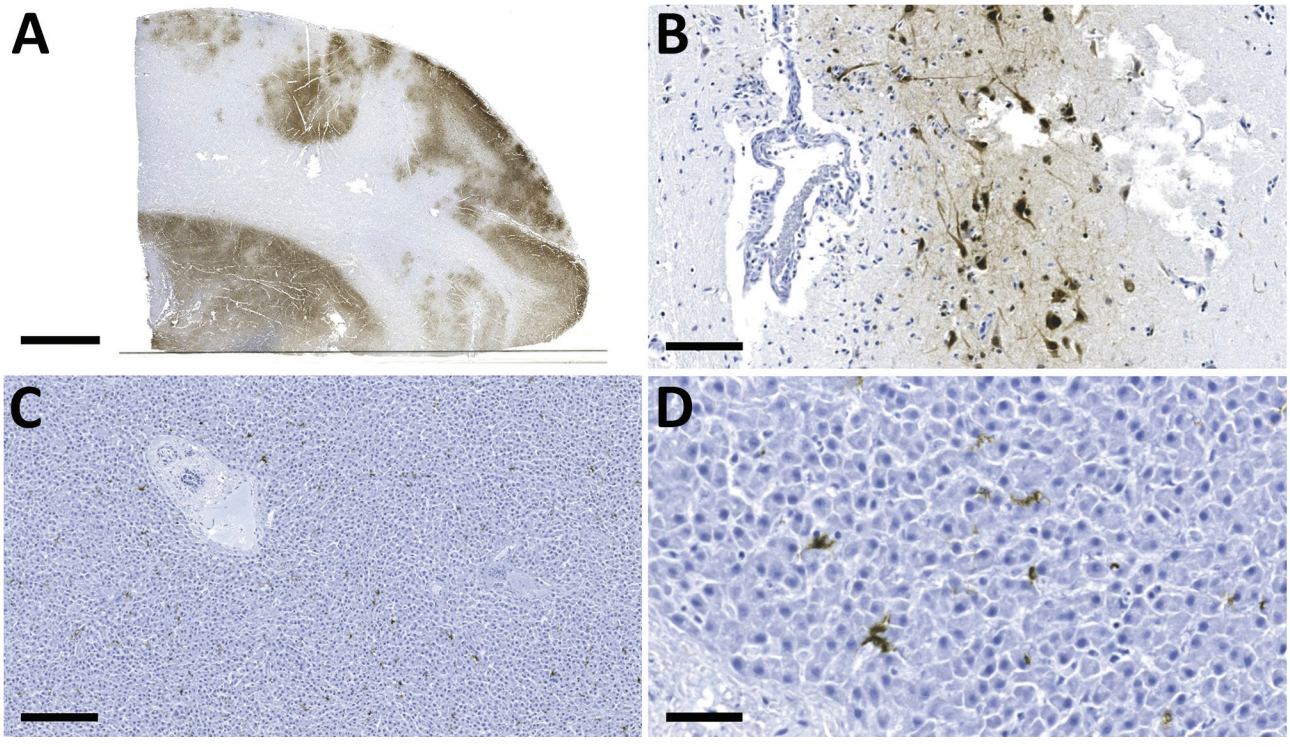

Figure 1. Detection of influenza A virus antigen in black bears by immunohistochemical analysis, Quebec, Canada. A) Brain tissue, showing abundant viral antigen detected multifocally throughout the section and observed primarily in gray matter areas. Scale bar indicates 5 mm. B) Brain immunostaining within neurons and surrounding neuropil. Scale bar indicates 100 μm. C) Liver tissue, showing viral antigen within individual cells. Scale bar indicates 200 μm. D) Liver tissue, showing that cells have the morphologic appearance of Kuppfer cells. Scale bar indicates 50 μm. Monoclonal antibody and diaminobenzidine stained, Gill's hematoxylin counterstained.

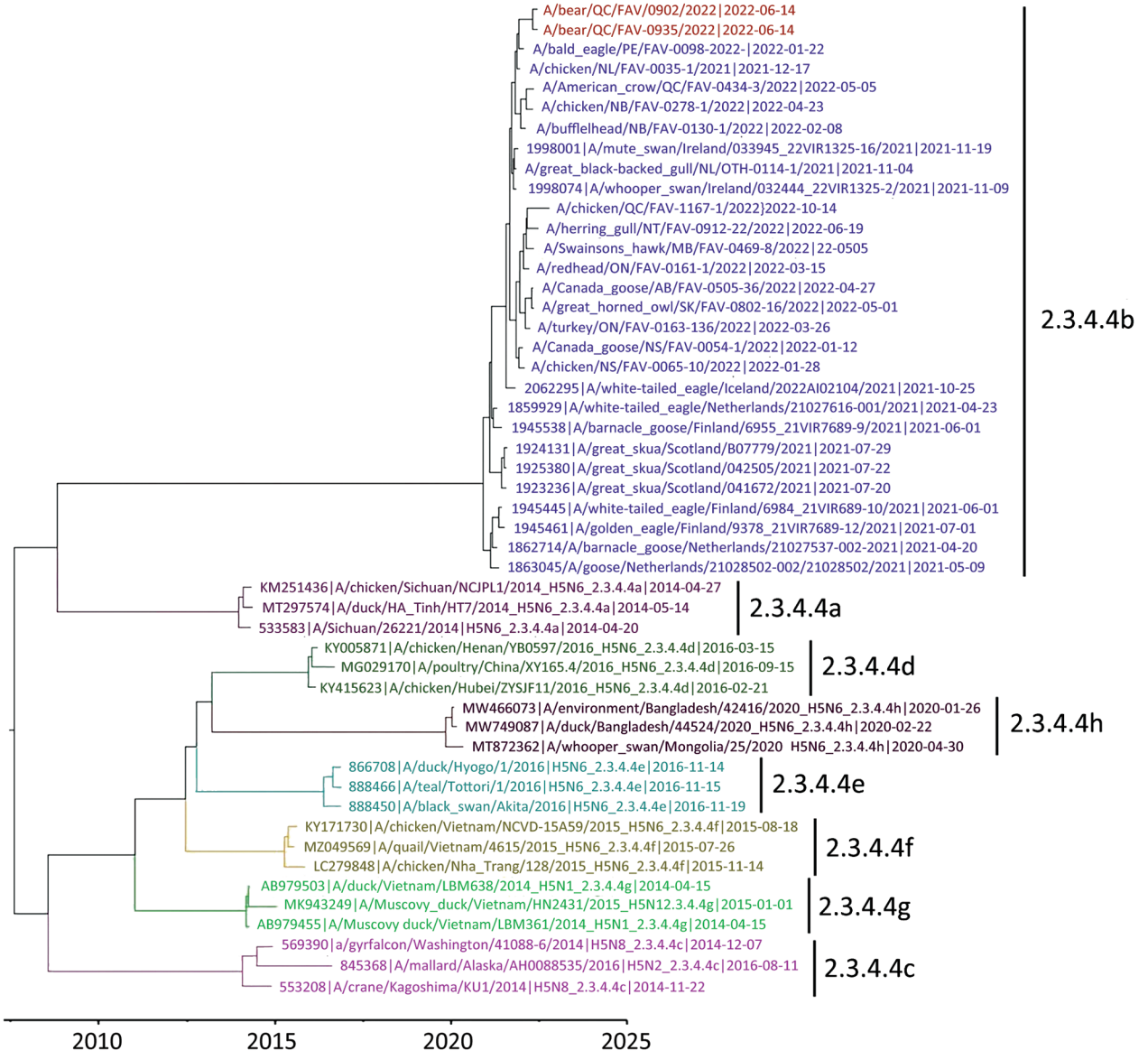

Figure 2. Maximum-clade credibility tree for influenza A virus antigen in black bears by immunohistochemical analysis, Quebec, Canada, inferred by using Bayesian and Markov Chain Monte Carlo analyses for the H5 hemagglutinin gene. Shown are relationships among black bear strains from this investigation (red), European 2021 H5 clade 2.3.4.4b HPAI strains (blue), and early Canada wild bird and poultry strains (purple). Colors and labels indicate the other H5 clade 2.3.4.4 subgroups.

Flyway in 2021 (*1*). Both bears had mammalian adaptive mutations (D701N) in the polymerase basic protein 2 subunit of the RNA polymerase complex.

We conducted a Bayesian phylogenetic analysis to identify phylogenetic relatedness of the H5 HA gene between black bears and Eurasian-origin H5N1 HPAIVs, as well as representative subgroups of clade 2.3.4.4. (Appendix). The maximum clade credibility tree of the H5 HA gene showed that the HA genes of black bear samples were grouped with the current outbreak 2.3.4.4b subgroup (Figure 2). The HA genes were most closely related to those of early H5N1 HPAIVs isolated from eastern Canada provinces, as well as strains circulating in northwestern Europe during winter 2021. Those genes were also more similar to those the fully Eurasian lineages observed in red foxes than to those observed in striped skunks and mink (*5*) and were not closely related to the New England–specific lineages documented in New England seals (*7*). Full genome sequences of both isolates were deposited in the GISAID database (https://www.gisaid.org) under accession nos. EPI_ISL_1747865 and EPI_ISL_17478584.

Conclusions

The described black bears were within the Atlantic Americas avian flyway, where Eurasian lineage H5N1 viruses were detected in 2021 (*1*). The global epizootic of the HPAI H5N1 virus belonging to clade 2.3.4.4b has led to an exceptional number of animal deaths, particularly in domestic poultry and wild birds (*12*).

As opportunistic omnivores, black bears might be found scavenging on carcasses of dead animals, including birds. Within 5 km and in the 3 weeks preceding the euthanasia of both bears, several dead wild birds tested positive for the Eurasian lineage of HPAI H5N1, including common murre (*Uria aalge*), American crow (*Corvus brachyrhynchos*), northern gannet (*Morus bassanus*), and razorbill (*Alca torda*) (Canadian Wildlife Health Cooperative internal database, https://www.cwhc-rcsf.ca). Suspected deaths of seals caused by HPAI H5N1 had occurred around the same time that the bears were found; however, those seal carcasses were >300 km away, and no suspected or confirmed seal deaths caused by HPAI H5N1 have been reported in seal populations in the Gaspé Peninsula (*13*). Therefore, it is suspected that the adult female black bear in this study was infected through spillover directly from infected bird carcasses because black bears in the Gaspé Peninsula share habitat with marine birds for which there have been confirmed deaths caused by HPAI H5N1 (*13*; Canadian Wildlife Health Cooperative internal database) during the same period.

Although H5N1 virus transmission has been documented in mink and ferrets, transmission of the virus between mammals is generally inefficient (*14*). Therefore, the possibility that the virus that affected these black bears was transmitted from 1 bear to another, or from another mammal species, is much less probable than transmission from birds. Although HPAI virus infections in mammals might occur secondary to other infections, no other infectious agents were identified in either of the black bears.

Acknowledgments

We thank the employees of the Complex de Diagnostic et d'Épidémiosurveillance Vétérinaire du Québec for their contributions and work, M. Fisher for sequencing and sequence data processing, and the Parks Canada wildlife officials for their involvement in this study.

Support was provided to O.L. by the Canadian Safety and Security Program (CSSP-2018-TA-2362) for the Oxford Nanopore GridION sequencer.

About the Author

Dr. Jakobek is a veterinary resident in wildlife health management with the Canadian Wildlife Health Cooperative and the Faculté de Médecine Vétérinaire at the Université de Montréal, Saint-Hyacinthe, Quebec, Canada. His primary research interests are wildlife disease epidemiology and conservation medicine.

References

1. Caliendo V, Lewis NS, Pohlmann A, Baillie SR, Banyard AC, Beer M, et al. Transatlantic spread of highly pathogenic avian influenza H5N1 by wild birds from Europe to North America in 2021. Sci Rep. 2022;12:11729. https://doi.org/10.1038/s41598-022-13447-z
2. Prosser DJ, Schley HL, Simmons N, Sullivan JD, Homyack J, Weegman M, et al. A lesser scaup (*Aythya affinis*) naturally infected with Eurasian 2.3.4.4 highly pathogenic H5N1 avian influenza virus: movement ecology and host factors. Transbound Emerg Dis. 2022;69:e2653–60. https://doi.org/10.1111/tbed.14614
3. Nemeth NM, Ruder MG, Poulson RL, Sargent R, Breeding S, Evans MN, et al. Bald eagle mortality and nest failure due to clade 2.3.4.4 highly pathogenic H5N1 influenza A virus. Sci Rep. 2023;13:191. https://doi.org/10.1038/s41598-023-27446-1
4. World Health Organization. Human infection with avian influenza A(H5) viruses. Avian Influenza Weekly Update Number 887.
5. Alkie TN, Cox S, Embury-Hyatt C, Stevens B, Pople N, Pybus MJ, et al. Characterization of neurotropic HPAI H5N1 viruses with novel genome constellations and mammalian adaptive mutations in free-living mesocarnivores in Canada. Emerg Microbes Infect. 2023;12:2186608. https://doi.org/10.1080/22221751.2023.2186608
6. Horimoto T, Maeda K, Murakami S, Kiso M, Iwatsuki-Horimoto K, Sashika M, et al. Highly pathogenic avian influenza virus infection in feral raccoons, Japan. Emerg Infect Dis. 2011;17:714–7. https://doi.org/10.3201/eid1704.101604
7. Puryear W, Sawatzki K, Hill N, Foss A, Stone JJ, Doughty L, et al. Highly of highly pathogenic avian influenza A (H5N1) in New England seals, United States. Emerg Infect Dis. 2023;29:786–91. https://doi.org/10.3201/eid2904.221538
8. Boedeker NC, Nelson MI, Killian ML, Torchetti MK, Barthel T, Murray S. Pandemic (H1N1) 2009 influenza A virus infection associated with respiratory signs in sloth bears (*Melursus ursinus*). Zoonoses Public Health. 2017;64:566–71. https://doi.org/10.1111/zph.12370
9. Saturday GA, King R, Fuhrmann L. Validation and operational application of a rapid method for rabies antigen detection. US Army Med Dep J. 2009;(Jan–Mar):42–5.
10. Spackman E, Senne DA, Myers TJ, Bulaga LL, Garber LP, Perdue ML, et al. Development of a real-time reverse transcriptase PCR assay for type A influenza virus and the avian H5 and H7 hemagglutinin subtypes. J Clin Microbiol. 2002;40:3256–60. https://doi.org/10.1128/JCM.40.9.3256-3260.2002
11. Weingartl HM, Berhane Y, Hisanaga T, Neufeld J, Kehler H, Emburry-Hyatt C, et al. Genetic and pathobiologic characterization of pandemic H1N1 2009 influenza viruses from a naturally infected swine herd. J Virol. 2010;84:2245–56. https://doi.org/10.1128/JVI.02118-09
12. Adlhoch C, Fusaro A, Gonzales JL, Kuiken T, Marangon S, Niqueux É, et al.; European Food Safety Authority; European

Centre for Disease Prevention and Control; European Union Reference Laboratory for Avian Influenza. Avian influenza overview December 2021–March 2022. EFSA J. 2022;20:e07289.
13. Canadian Food Inspection Agency, National Emergency Operation Centre, Geographic Information System Services. Highly pathogenic avian influenza—wild birds [cited 2023 Apr 11]. https://cfia-ncr.maps.arcgis.com/apps/dashboards/89c779e98cdf492c899df23e1c38fdbc
14. Imai M, Herfst S, Sorrell EM, Schrauwen EJA, Linster M, De Graaf M, et al. Transmission of influenza A/H5N1 viruses in mammals. Virus Res. 2013;178:15–20. https://doi.org/10.1016/j.virusres.2013.07.017

Address for correspondence: Stéphane Lair, Centre Québécois sur la Santé des Animaux Sauvages/Canadian Wildlife Health Cooperative, Faculté de Médecine Vétérinaire, Université de Montréal, 3200 Rue Sicotte, St. Hyacinthe, QB J2S 2M2, Canada; email: stephane.lair@umontreal.ca

Article DOI: https://doi.org/10.3201/eid2910.230548

Influenza A(H5N1) Virus Infections in 2 Free-Ranging Black Bears (*Ursus americanus*), Quebec, Canada

Appendix

Materials and Methods

Phylogenetic Analysis

The H5 HA genes of two black bear samples were aligned with HA genes of Eurasian origin H5N1 HPAIVs as well as representative subgroups of clade 2.3.4.4 by using MUSCLE (*1*), and alignments were trimmed to contain coding regions. A Bayesian phylogenetic analysis was conducted to show phylogenetic relatedness by using a Bayesian Markov Chain Monte Carlo (BMCMC) method (*2*) as implemented in the BEAST 2 program version 2.7.4 (*3*). The GTR + G nucleotide substitution model was applied to the dataset for Bayesian analysis. The age of the viruses was defined as the date of sample collection from the dataset. The coalescent Bayesian skyline was used for tree prior and an uncorrelated log-normal relaxed clock model was used to reflect the complex population dynamics of AIVs. For the dataset, at least two independent BEAST analysis runs were conducted for 30 million generations, sampling every 3000 generations. Convergences and effective sample sizes (ESS) of the estimates were checked by using Tracer v1.7.2 (http://tree.bio.ed.ac.uk/software/tracer). All parameter estimates for each run showed ESS values >200. A maximum clade credibility (MCC) phylogenetic tree was generated to summarize all 10,000 trees after a 10% burn-in by using TreeAnnotator in BEAST 2 (*4*). The time-stamped phylogenetic tree was visualized and annotated by using FigTree v1.4.4 (http://tree.bio.ed.ac.uk/software/figtree).

Immunohistochemistry

For immunohistochemistry, paraffin tissue sections were quenched for 10 minutes in aqueous 3% hydrogen peroxide. Epitopes were then identified by using proteinase K for 15 minutes, then rinsed.

The primary antibody applied to the sections was a mouse monoclonal antibody specific for influenza A nucleoprotein (NP) (F26NP9, produced in-house) and was used at a dilution of 1:5,000 for 30 minutes. They were then visualized by using a horse radish peroxidase–labeled polymer, EnVision+ System (anti-mouse) (Dako, USA) and reacted with the chromogen diaminobenzidine (DAB). The sections were then counter stained with Gill's hematoxylin.

References

1. Edgar RC. MUSCLE: multiple sequence alignment with high accuracy and high throughput. Nucleic Acids Res. 2004;32:1792–7. PubMed https://doi.org/10.1093/nar/gkh340

2. Drummond AJ, Nicholls GK, Rodrigo AG, Solomon W. Estimating mutation parameters, population history and genealogy simultaneously from temporally spaced sequence data. Genetics. 2002;161:1307–20. PubMed https://doi.org/10.1093/genetics/161.3.1307

3. Bouckaert R, Vaughan TG, Barido-Sottani J, Duchêne S, Fourment M, Gavryushkina A, et al. BEAST 2.5: an advanced software platform for Bayesian evolutionary analysis. PLOS Comput Biol. 2019;15:e1006650. PubMed https://doi.org/10.1371/journal.pcbi.1006650

4. Drummond AJ, Suchard MA, Xie D, Rambaut A. Bayesian phylogenetics with BEAUti and the BEAST 1.7. Mol Biol Evol. 2012;29:1969–73. PubMed https://doi.org/10.1093/molbev/mss075

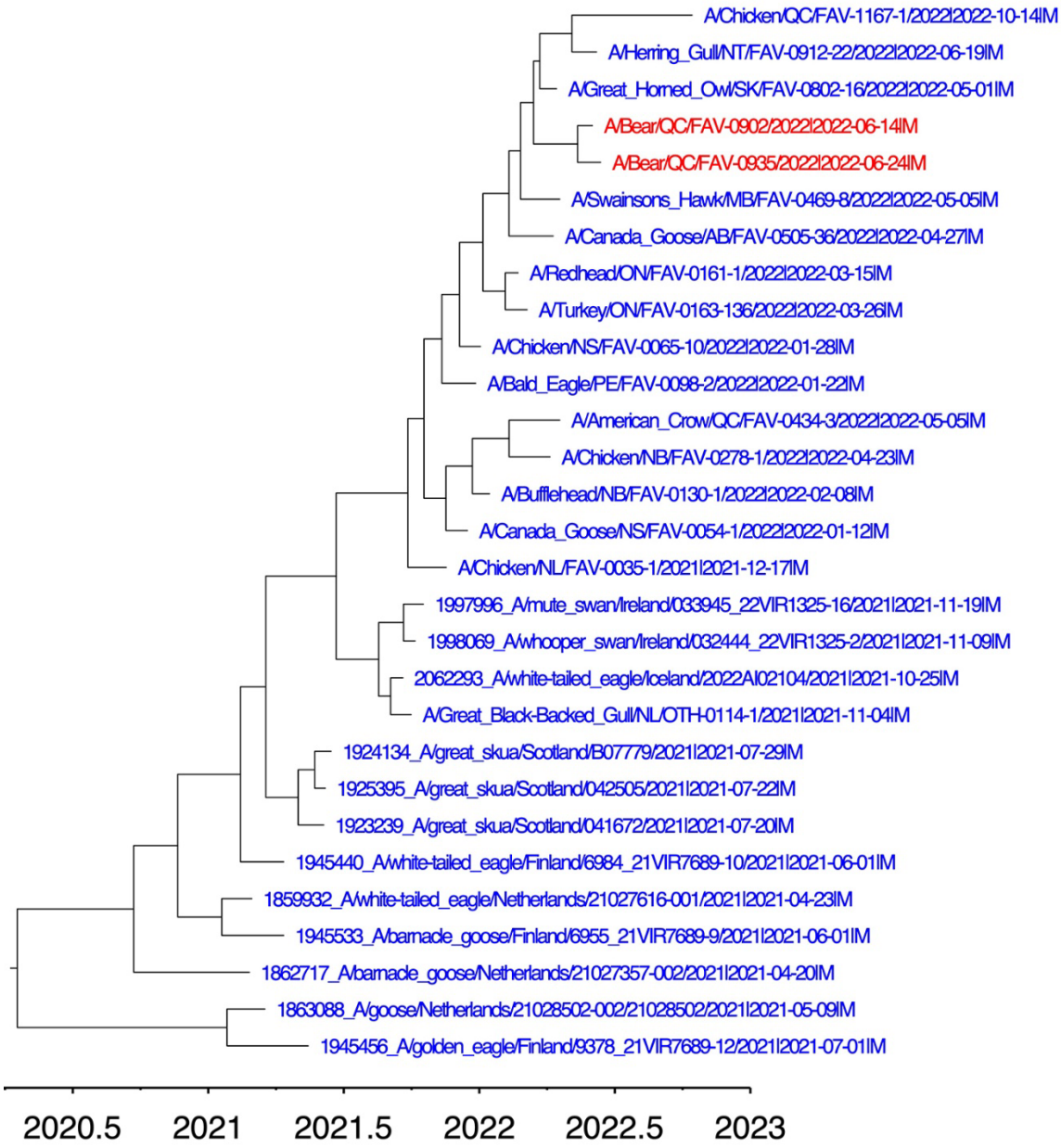

Appendix Figure 1. M (nt = 982) nucleotides from maximum clade credibility (MCC) tree inferred using Bayesian Markov Chain Monte Carlo (BMCMC) analysis for additional genomic segments from 29 strains described in 2.3.4.4b clade of Figure 2. Relationships among the European 2021 H5 2.3.4.4b HPAI strains (blue), the early Canadian wild birds and poultry strains (blue), and black bear strains (red).

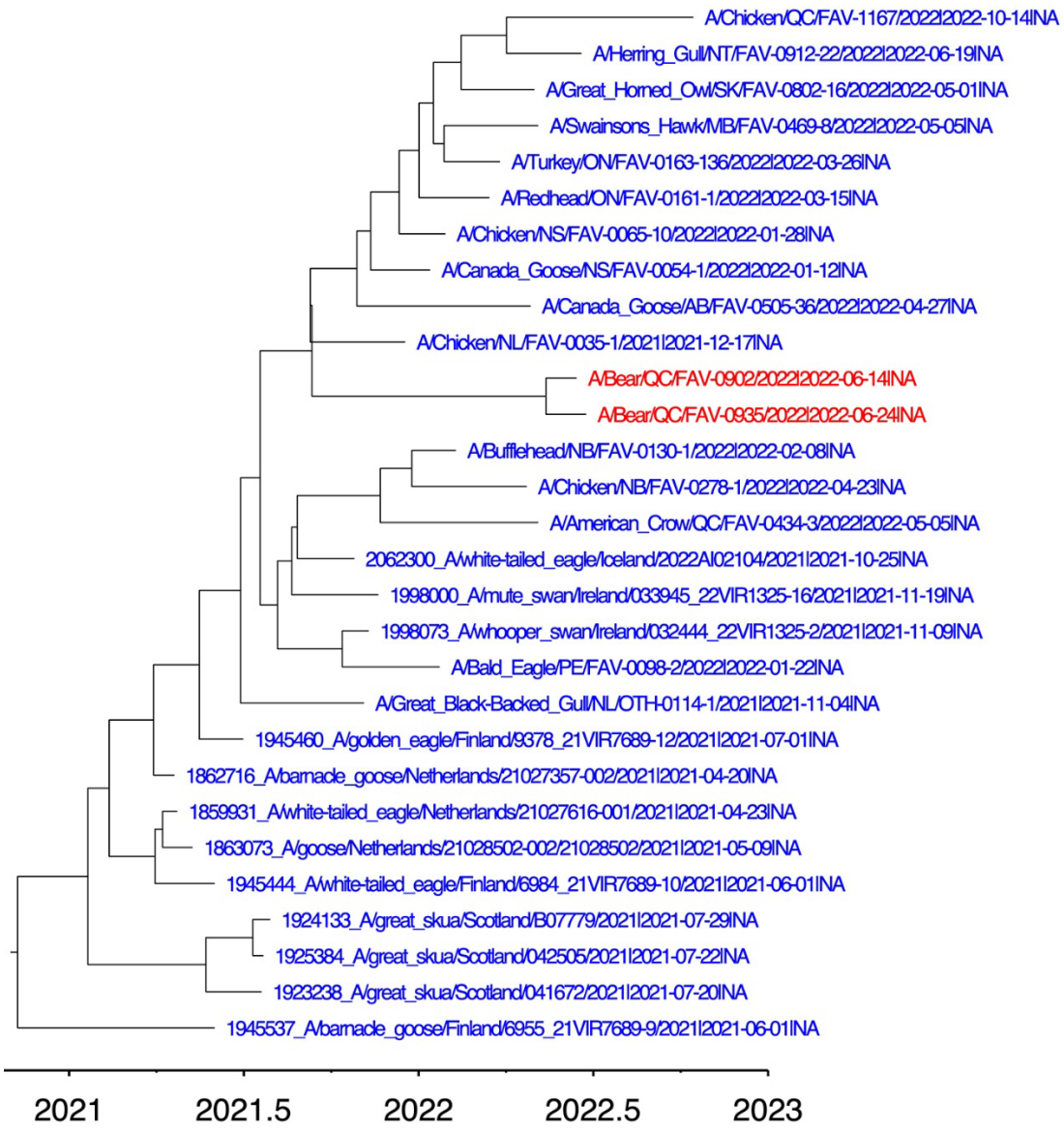

Appendix Figure 2. NA (nt = 1410) nucleotides from maximum clade credibility (MCC) tree inferred using Bayesian Markov Chain Monte Carlo (BMCMC) analysis for additional genomic segments from 29 strains described in 2.3.4.4b clade of Figure 2. Relationships among the European 2021 H5 2.3.4.4b HPAI strains (blue), the early Canadian wild birds and poultry strains (blue), and black bear strains (red).

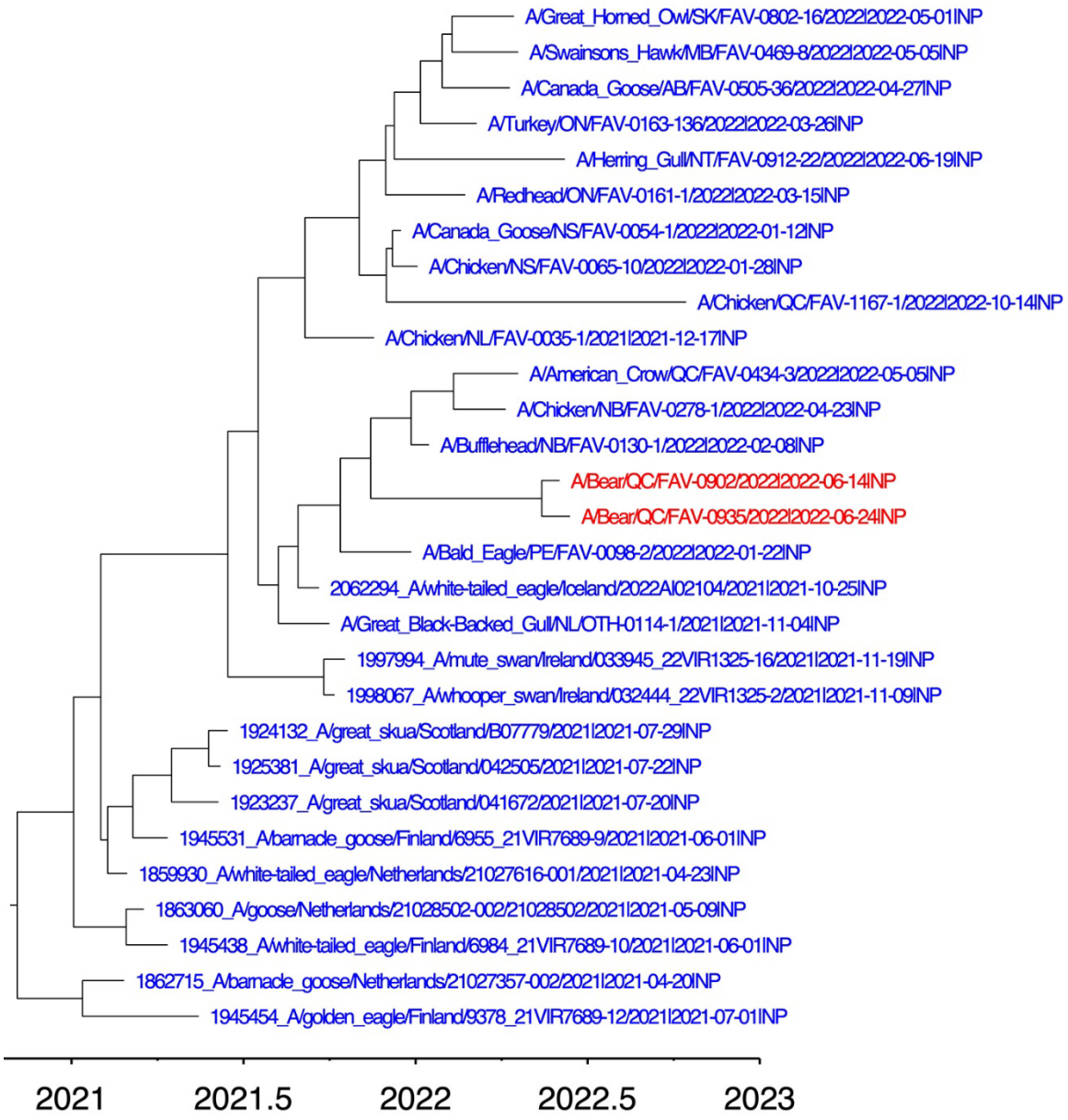

Appendix Figure 3. NP (nt = 1497) nucleotides from maximum clade credibility (MCC) tree inferred using Bayesian Markov Chain Monte Carlo (BMCMC) analysis for additional genomic segments from 29 strains described in 2.3.4.4b clade of Figure 2. Relationships among the European 2021 H5 2.3.4.4b HPAI strains (blue), the early Canadian wild birds and poultry strains (blue), and black bear strains (red).

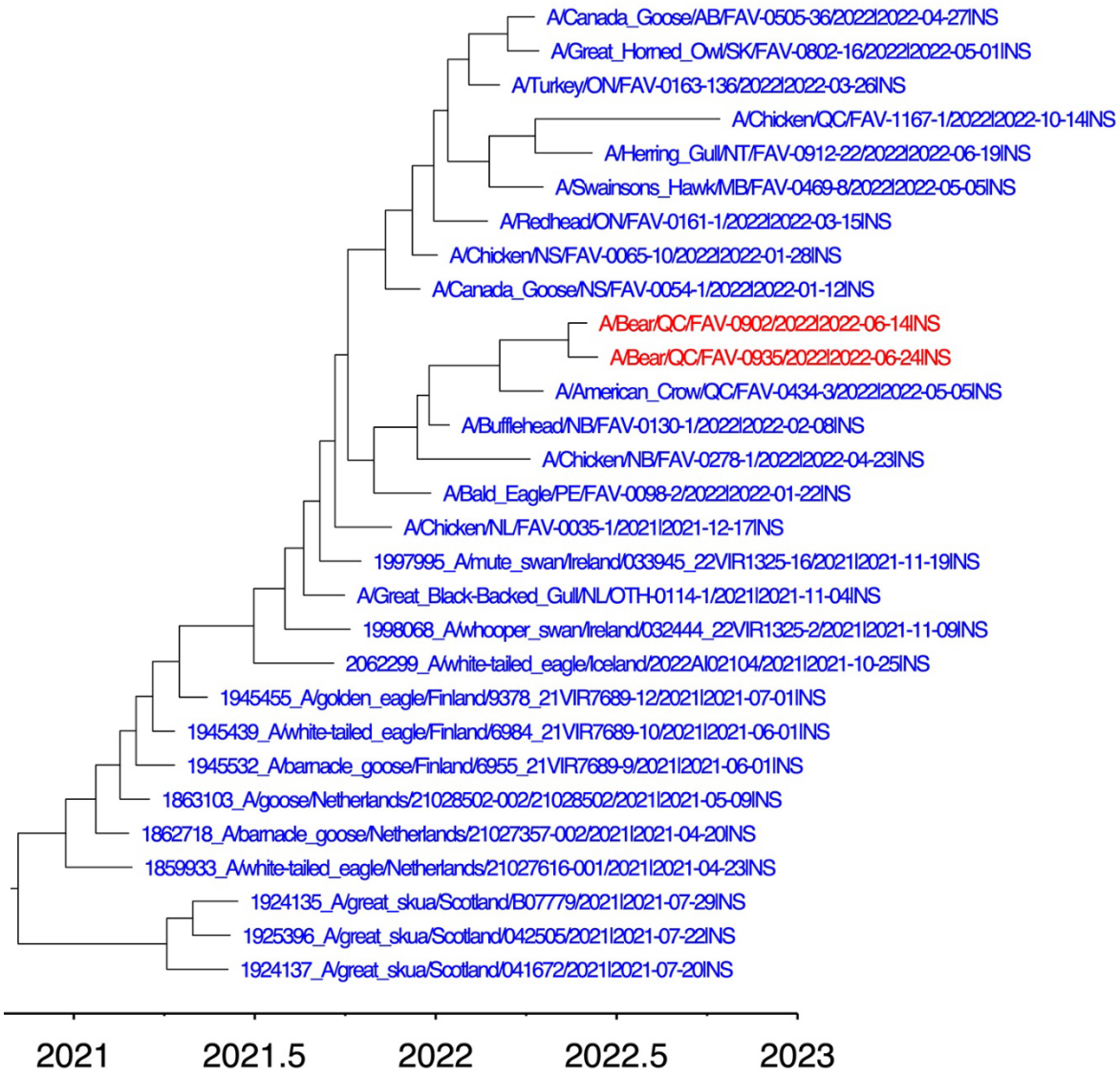

Appendix Figure 4. NS (nt = 838) nucleotides from maximum clade credibility (MCC) tree inferred using Bayesian Markov Chain Monte Carlo (BMCMC) analysis for additional genomic segments from 29 strains described in 2.3.4.4b clade of Figure 2. Relationships among the European 2021 H5 2.3.4.4b HPAI strains (blue), the early Canadian wild birds and poultry strains (blue), and black bear strains (red).

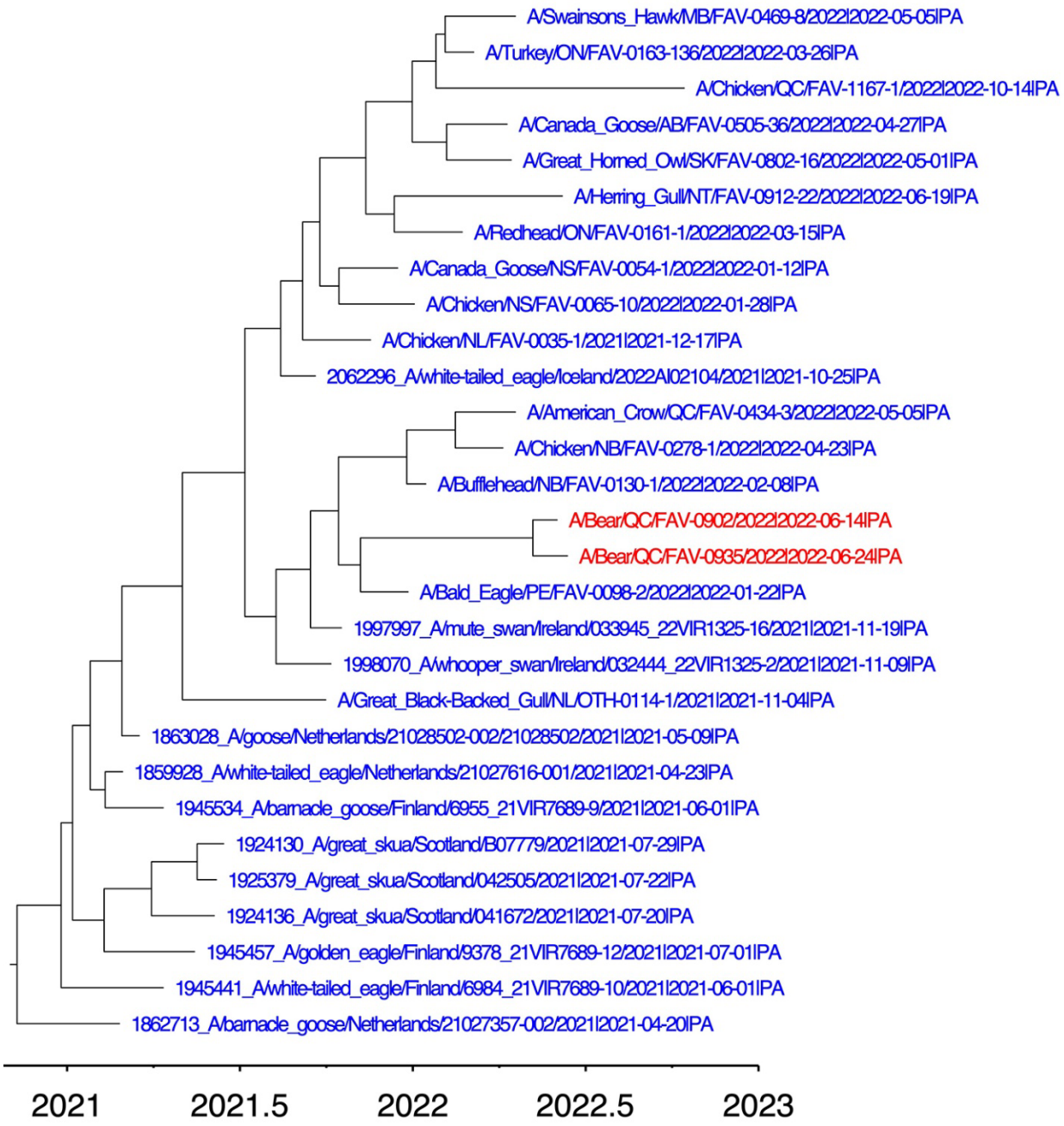

Appendix Figure 5. PA (nt = 2151) nucleotides from maximum clade credibility (MCC) tree inferred using Bayesian Markov Chain Monte Carlo (BMCMC) analysis for additional genomic segments from 29 strains described in 2.3.4.4b clade of Figure 2. Relationships among the European 2021 H5 2.3.4.4b HPAI strains (blue), the early Canadian wild birds and poultry strains (blue), and black bear strains (red).

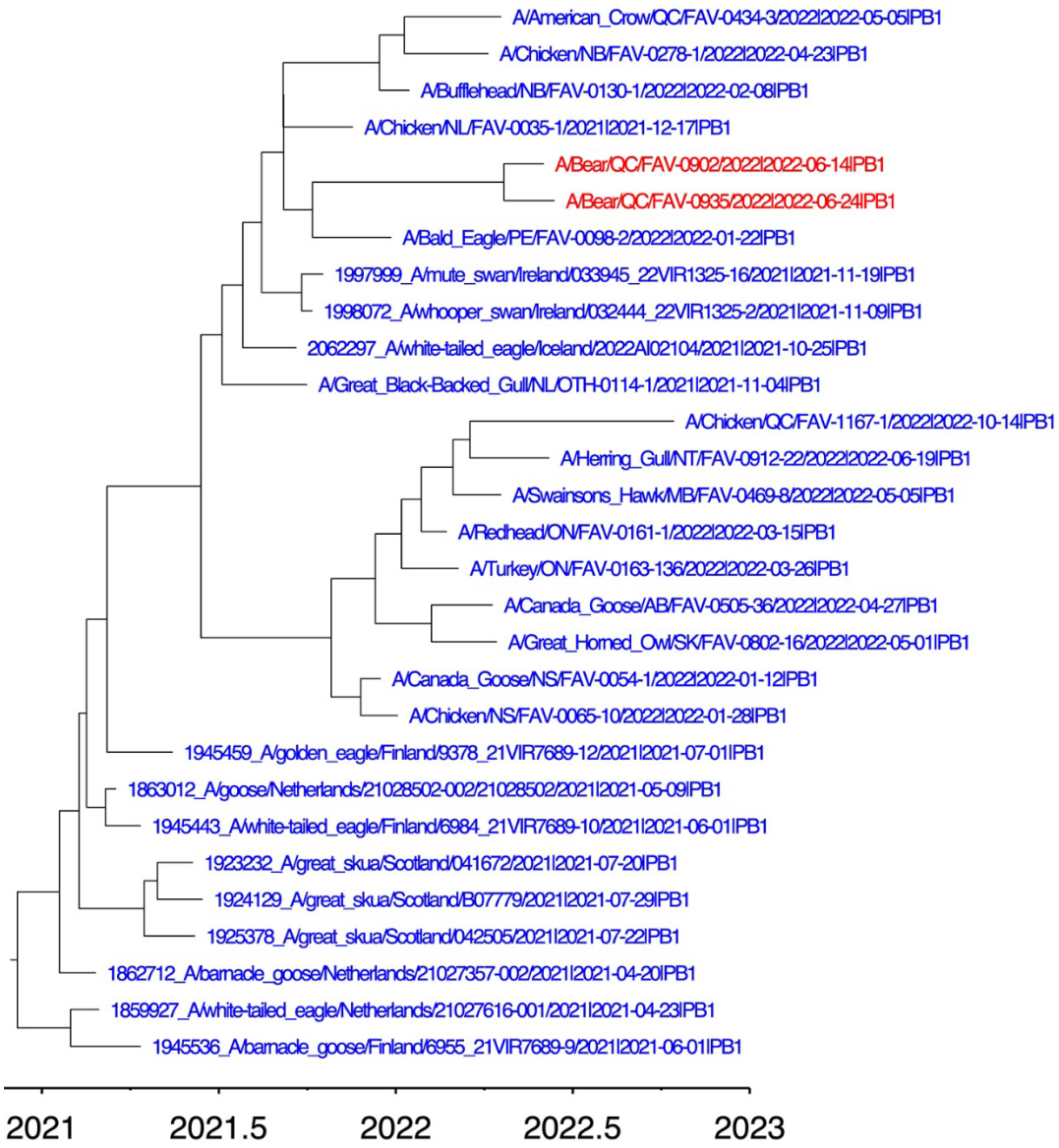

Appendix Figure 6. PB1 (nt = 2274) nucleotides from maximum clade credibility (MCC) tree inferred using Bayesian Markov Chain Monte Carlo (BMCMC) analysis for additional genomic segments from 29 strains described in 2.3.4.4b clade of Figure 2. Relationships among the European 2021 H5 2.3.4.4b HPAI strains (blue), the early Canadian wild birds and poultry strains (blue), and black bear strains (red).

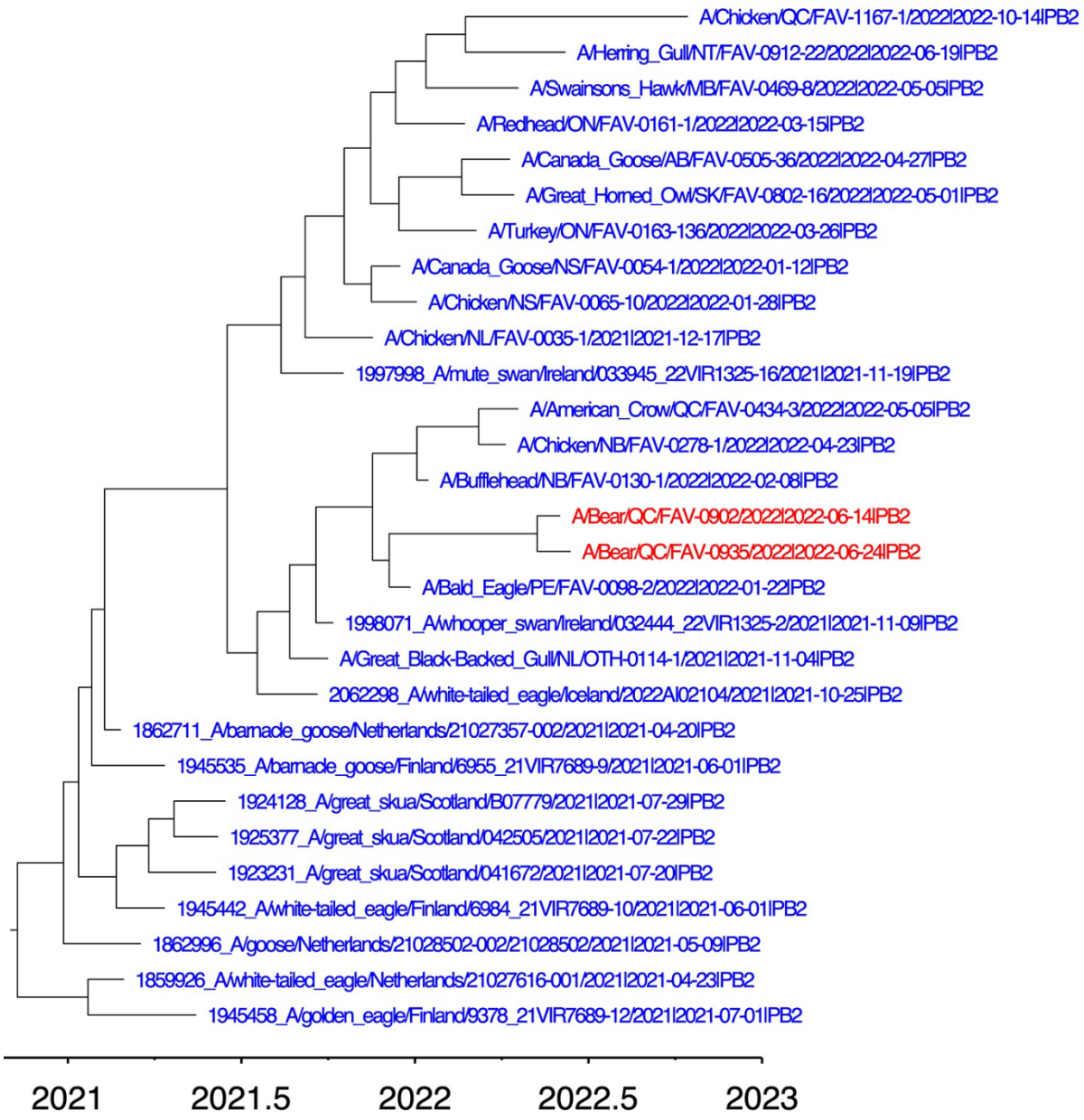

Appendix Figure 7. PB2 (nt = 2280) nucleotides from maximum clade credibility (MCC) tree inferred using Bayesian Markov Chain Monte Carlo (BMCMC) analysis for additional genomic segments from 29 strains described in 2.3.4.4b clade of Figure 2. Relationships among the European 2021 H5 2.3.4.4b HPAI strains (blue), the early Canadian wild birds and poultry strains (blue), and black bear strains (red).